analytical chemistry

Article

pubs.acs.org/ac

Long-Term Real-Time Monitoring Catalytic Synthesis of Ammonia in a Microreactor by VUV-Lamp-Based Charge-Transfer Ionization Time-of-Flight Mass Spectrometry

Yuanyuan Xie,[†,‡] Lei Hua,[†] Keyong Hou,[†] Ping Chen,[†,‡] Wuduo Zhao,[†,‡] Wendong Chen,[†,‡] Bangyu Ju,[†] and Haiyang Li*[,†]

[†]Key Laboratory of Separation Science for Analytical Chemistry, Dalian Institute of Chemical Physics, Chinese Academy of Sciences, 457 Zhongshan Road, Dalian, 116023, People's Republic of China

[‡]Graduate University of Chinese Academy of Sciences, 19 Yuquan Road, Beijing, 100039, People's Republic of China

Supporting Information

ABSTRACT: With respect to massive consumption of ammonia and rigorous industrial synthesis conditions, many studies have been devoted to investigating more environmentally benign catalysts for ammonia synthesis under moderate conditions. However, traditional methods for analysis of synthesized ammonia (e.g., off-line ion chromatography (IC) and chemical titration) suffer from poor sensitivity, low time resolution, and sample manipulations. In this work, charge-transfer ionization (CTI) with O_2^+ as the reagent ion based on a vacuum ultraviolet (VUV) lamp in a time-of-flight mass spectrometer (CTI-TOFMS) has been applied for real-time monitoring of the ammonia synthesis in a microreactor. For the necessity of long-term stable monitoring, a self-adjustment algorithm for stabilizing O_2^+ ion intensity was developed to automatically compensate the attenuation of the O_2^+ ion yield in the ion source as a result of the oxidation of the photoelectric electrode and contamination on the MgF_2 window of the VUV lamp. A wide linear calibration curve in the concentration range of 0.2−1000 ppmv with a correlation coefficient (R^2) of 0.9986 was achieved, and the limit of quantification (LOQ) for NH_3 was in ppbv. Microcatalytic synthesis of ammonia with three catalysts prepared by transition-metal/carbon nanotubes was tested, and the rapid changes of NH_3 conversion rates with the reaction temperatures were quantitatively measured with a time resolution of 30 s. The high-time-resolution CTI-TOFMS could not only achieve the equilibrium conversion rates of NH_3 rapidly but also monitor the activity variations with respect to investigated catalysts during ammonia synthesis reactions.

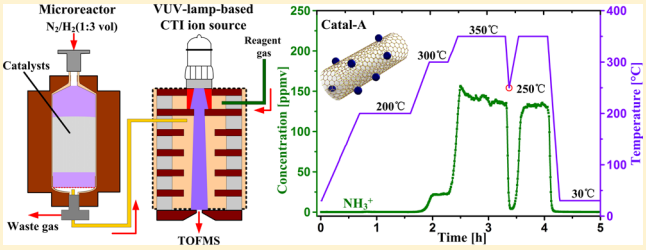

The massive consumption of ammonia for agricultural and industrial use has impelled humankind to continuously increase the ammonia production. Industrially, the Haber−Bosch process is the main route to produce ammonia.[1,2] However, this process requires rigorous reaction conditions and consumes 1−2% of the world's annual energy supply with a significant amount of carbon dioxide released.[3,4] Therefore, many studies have been focused on investigating more environmentally benign catalysts for microcatalytic synthesis of ammonia under milder conditions.[5−11] For example, transition-metal−N_2 complexes have been investigated to catalyze N_2 into NH_3 under ambient conditions.[5,6] Bacterial nitrogenase enzymes have been verified to produce NH_3 through biological N_2 fixation under ambient temperature and pressure.[7−9] Some methods have been reported for measurement of the effluent ammonia during these synthesis microreactions (e.g., ion chromatography (IC)[10] and chemical titration).[5,6,12,13] Because of its poor sensitivity and off-line sample preparation, time resolution of the IC ranged from 2 to 25 h with a total of 35 mmol ammonia produced in a catalytic reaction of 75 h.[10] As anticipated for IC, the low-time-resolution data bears the risk of missing rapid and important information about the catalytic activity of studied catalysts. The chemical titration method suffers from the same disadvantage of low time resolution. Besides, because chemical titration is established on the basis of visual perception of the changes of solution color, there is a high experimenter-to-experimenter variance of results especially for ammonia with low concentration. Therefore, development of high-time-resolution and more sensitive techniques for evolved ammonia analysis becomes necessary to evaluate the catalytic efficiency of the catalysts and monitor the activity changes induced by reaction parameters.

Online mass spectrometry (MS) is gaining widespread use to monitor catalytic dynamic processes without unnecessary interruptions and sample preparations.[14−18] For traditional electron impact ionization (EI), NH_3^+ ions are formed by ionizing NH_3. However, the neutral molecule H_2O could be

Received: April 30, 2014
Accepted: June 26, 2014
Published: June 26, 2014

   dx.doi.org/10.1021/ac501576f | Anal. Chem. 2014, 86, 7681−7687

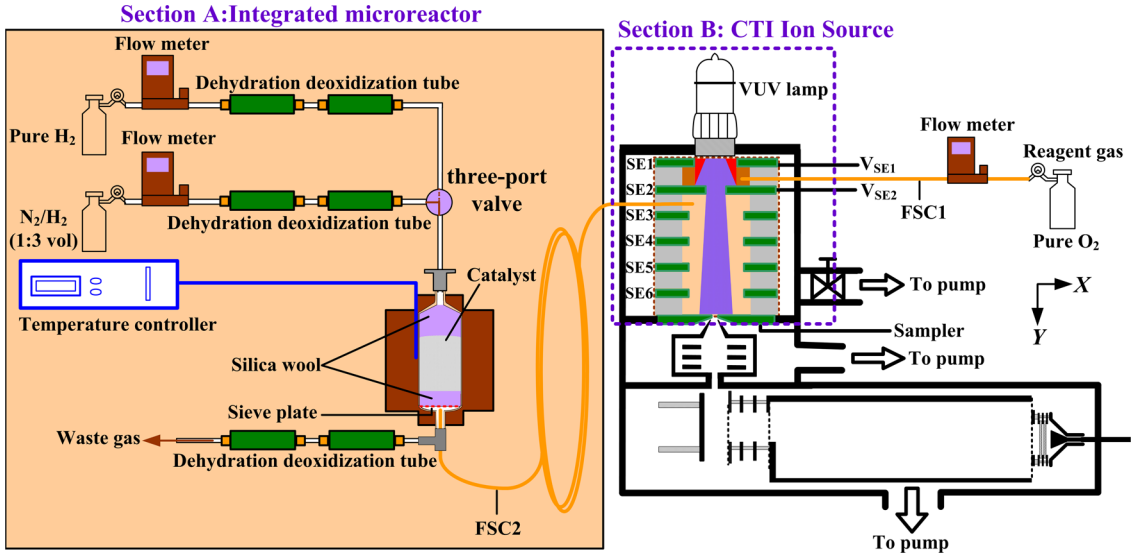

Figure 1. Schematic diagram of the integrated microreactor and the VUV-lamp-based O_2^+ charge-transfer ionization source coupled with an orthogonal acceleration time-of-flight mass spectrometer.

ionized by EI to generate HO^+ ions with a relative intensity of 20%, which interferes with the identification of NH_3^+.[19] Moreover, the pressure in the EI source has to be kept as low as possible to prolong the lifetime of the heated filament, which restricted further improvement of the sensitivity. Under high vacuum condition of 10^{-4} Pa in an EI source, 25 ppmv NH_3 failed to achieve obvious response at $m/z = 17$ (see Figure S-1 in Supporting Information).

Various soft ionization techniques (e.g., proton transfer reaction (PTR), single-photon ionization (SPI) and chemical ionization (CI)), may meet the requirement for ammonia analysis. The higher proton affinity (PA) of NH_3 (853.6 kJ mol^{-1}) than H_2O (691 kJ mol^{-1}) makes it possible to measure NH_3 by PTR-MS, which is based on proton transfer reaction with H_3O^+ to form NH_4^+ ions. PTR-MS[20,21] was reported to determine ammonia in the atmosphere. However, the PTR-MS instrument suffers from a high instrumental background (typically several 10^4 cps of NH_4^+ ions) as a result of intrinsic formation of NH_3 from H_2O and N_2 in the hollow cathode ion source.[21] Moreover, H_2O^+ will interfere with the identification and quantification of NH_4^+ because of overlapping peaks in spectra.[22]

SPI has been applied for analysis of complex samples (e.g., diesel fuel,[23,24] cigarette smoke,[25,26] and volatile organic compounds (VOCs)[27−29]). However, limited by the photon flux of the VUV lamp (1.0×10^{11} photons s^{-1}) and small photoionization cross-section of NH_3 (1.3×10^{-18} cm^2 at 118 nm),[30] the achievable sensitivity of NH_3 by VUV-lamp-based SPI-MS is not satisfactory. Additionally, the photon flux of the VUV lamp may decay in vacuum as a result of contamination on the MgF_2 window of the VUV lamp, which needs sequential external calibration for long-time continuous operation.[31]

Recently, Li et al.[27,32] developed VUV-lamp-based charge-transfer ionization ion source time-of-flight mass spectrometry (CTI-TOFMS). The VUV-lamp-based CTI ion source not only expanded the obtainable information considerably but also improved the analytical sensitivity of compounds with ionization energies below the VUV photon energy (10.6 eV). In CTI mode, O_2^+ reagent ions were generated by photoelectron ionization (PEI) of pure O_2 gas. The recombination energy of O_2^+ is 12.07 eV, the ionization energy of NH_3 is 10.07 eV, so the charge transfer from O_2^+ to NH_3 is valid and efficient with product ion of NH_3^+.[21] CTI-MS based on a PTR-MS instrument operated with pure O_2 as reagent gas has been successfully applied for measurement of atmospheric NH_3, even at low ppbv level.[21,33,34]

The present work describes the combination of a CTI-TOFMS to an integrated microreactor for real-time monitoring of the microcatalytic ammonia synthesis reaction with a time resolution of 30 s. A self-adjustment algorithm was designed to compensate the attenuation of the VUV lamp and the oxidation of the photoelectric electrode for long-term monitoring and wide quantification range. As a result, stable continuous monitoring of ammonia microsynthesis reactions could last at least 50 h.

EXPERIMENTAL SECTION

The apparatus for online monitoring of ammonia microsynthesis consists of an integrated microreactor device and a VUV-lamp-based charge-transfer ionization ion source coupled with a home-built orthogonal acceleration time-of-flight mass spectrometer (CTI-TOFMS), as shown in Figure 1.

VUV-Lamp-Based CTI Ion Source. Full details of the VUV-lamp-based CTI ion source have been reported before.[27] Thus, only a brief description is given here. The CTI ion source as shown in section B of Figure 1 includes a commercial VUV krypton discharge lamp (10.6 eV, Cathodeon Ltd., Cambridge, U.K.) and an ionization cavity. The ionization cavity was made by six 1 mm thick stainless steel electrodes (SE1−SE6) and six 5 mm thick PTFE insulation washers. SE2 separated the ionization cavity into two regions: reagent ion-producing region between VUV lamp and SE2 electrode, ion−molecule reaction region between SE2 electrode and sampler electrode. The reagent gas O_2 and the effluent gas from microreactor were directly introduced into the reagent ion-producing region and the ion−molecule reaction region by a 250 μm i.d. 0.5 m long deactivated fused-silica capillary (FSC1) and a 200 μm i.d. 0.5 m long deactivated fused-silica capillary (FSC2), respectively. The pressure in the ion source was maintained at 40 Pa by a 3.5 L/s dry scroll pump (Agilent Technologies Inc., California,

dx.doi.org/10.1021/ac501576f | Anal. Chem. 2014, 86, 7681−7687

U.S.A.), and the variation of the pressure was less than 0.4 Pa during microcatalytic reactions.

The ion source could work at two different operation modes, SPI and CTI modes, by simply adjusting the voltage of SE1 (V_{SE1}) while keeping the voltages on other electrodes unchanged. In SPI mode, V_{SE1} was set at 30 V to hinder the PEI of the reagent molecules, and NH_3 was mainly ionized by the VUV photons. In CTI mode, V_{SE1} was set higher than 40 V so that the photoelectrons emitted from the SE2 electrode surface (as shown in eq 1) could ionize O_2 efficiently through eq 2.[35,36] The O_2^+ reagent ions were then transferred to the ion−molecule reaction region where NH_3 molecules were ionized through the charge-transfer reaction, as described in eq 3. The voltages of SE2 electrode (V_{SE2}) and the sampler electrode were maintained at 18 and 7 V, respectively.

$$\text{metal} + h\nu \rightarrow e^- \tag{1}$$

$$e^- + O_2 \rightarrow O_2^+ \tag{2}$$

$$O_2^+ + NH_3 \rightarrow NH_3^+ + O_2 \tag{3}$$

Kinetic Model of Charge-Transfer Reaction. In charge-transfer reaction, the changes with time of the number densities of O_2^+ reagent ions $[O_2^+]_t$ and NH_3^+ product ions $[NH_3^+]_t$ in the ion source are described by the following kinetic equations[37]

$$\frac{d[O_2^+]_t}{dt} = -[O_2^+]_t \frac{D_{P(O_2^+)}}{\Lambda^2} - [O_2^+]_t k[NH_3] \tag{4}$$

$$\frac{d[NH_3^+]_t}{dt} = -[NH_3^+]_t \frac{D_{P(NH_3^+)}}{\Lambda^2} + [O_2^+]_t k[NH_3] \tag{5}$$

Here k is the rate coefficient of eq 3 with an experimental datum of 1.0×10^{-9} cm^3 s^{-1}.[38] $[NH_3]$ is the number density of the NH_3 molecules in the ion source with calculated results of 5.66×10^8 cm^{-3} to 2.83×10^{12} cm^{-3}, corresponding to 0.2−1000 ppmv NH_3 in sample gas (see the Supporting Information S-2 for detailed calculation equation).[37] $D_{P(O_2^+)}$ and $D_{P(NH_3^+)}$ are the diffusion coefficients of the O_2^+ reagent ions and the NH_3^+ ions with calculated results of 602 cm^2 s^{-1} and 729 cm^2 s^{-1} at 298 K and 40 Pa, respectively.[39] Λ is the characteristic diffusion length of the ion source determined from only its dimensions, and Λ^2 is 6.22×10^{-2} cm^2 for CTI ion source.[40]

An exact solution of eq 4 and eq 5 gives the relationship between the product and the reagent ion number densities as[37,41]

$$[NH_3^+]_t = k[O_2^+]_t[NH_3]t \frac{\exp\left(k[NH_3]t + \frac{D_{P(O_2^+)} - D_{P(NH_3^+)}}{\Lambda^2}t\right) - 1}{k[NH_3]t + \frac{D_{P(O_2^+)} - D_{P(NH_3^+)}}{\Lambda^2}t} \tag{6}$$

For the continuously formed NH_3^+ ions, their residence time in the ion source varies from zero up to the total reaction time t_r. t_r is calculated to be 3.3×10^{-5} s from the reduced near-zero-field mobility K (2.45×10^4 cm^2 V^{-1} s^{-1}),[39] the electric field strength in the ion−molecule reaction region (3.67 V cm^{-1}), and the length of the ion−molecule reaction region (30 mm).[42] Thus, for $t = t_r$, eq 6 can be expressed as

$$[NH_3^+]_{t_r} = k[O_2^+]_{t_r}[NH_3]t_r D_e \tag{7}$$

where D_e, defined as the differential diffusion enhancement coefficient, is used to describe the effect of the differential diffusion and expressed as

$$D_e = \frac{\exp\left(k[NH_3]t_r + \frac{D_{P(O_2^+)} - D_{P(NH_3^+)}}{\Lambda^2}t_r\right) - 1}{k[NH_3]t_r + \frac{D_{P(O_2^+)} - D_{P(NH_3^+)}}{\Lambda^2}t_r} \tag{8}$$

For NH_3 with a concentration of 0.2 ppmv to 1000 ppmv, D_e varies from 0.9671 to 1.0131 with a small variation of 4.76%, and the diffusions of the ions impose little influence on the number density of the NH_3^+ ions. Thus, according to eq 7, stabilizing the number density of the O_2^+ ions is essential to obtain a steady response of the NH_3^+ ions and wide linear concentration range by charge-transfer ionization.

Combination of the Integrated Microreactor and CTI-TOFMS. The integrated microreactor, as shown in section A of Figure 1, includes a vertical quartz tube microreactor with an inner diameter of about 8 mm and a temperature controller. Both ends of the microreactor were filled with silica wool, and 100 mg of catalyst was placed between the silica wools. The CTI-TOFMS was coupled to the microreactor through FSC2, which was inserted just underneath the silica wool to reach a dead volume of about 0.2 mL. The sampling rate of TOFMS through FSC2 was 15 mL min^{-1}, so the dead time was about 0.5 s, and real-time monitoring was realized. The feed gas N_2/H_2 1:3 (vol), dehydrated by 5A type high strength molecular sieve (Dalian Sheng Mai Company, Dalian, China) and deoxygenated by 401 type Deoxidizer (Dalian Sheng Mai Company, Dalian, China), passed through the catalyst bed with a flow rate of 20 mL min^{-1}, and the excess gas was exhausted after dehydration and deoxidization treatment.

The TOF mass analyzer was operated in linear mode with a mass resolution of 900 (fwhm) at m/z = 78. The data were recorded with 30 s for a single analysis by a 100 ps time-to-digital converter (TDC) (model 9353, Ametek, Inc., Oak Ridge, TN, U.S.A.) at a repetition rate of 33 kHz. All the microcatalytic reactions were operated at atmospheric pressure, and the temperature-programmed procedures for the catalysts are listed in table S-1 of the Supporting Information.

Sample Preparation. Two ammonia standard gas mixtures with concentrations of 25 ppmv and 5000 ppmv in N_2/H_2 1:3 (vol) (Dalian Special Gas Company, Dalian, China) were further diluted with N_2/H_2 1:3 (vol) to a series of lower concentrations by using mass flow controllers. The purity of all gases was 99.999%. Three catalysts based on transition metals, provided by State Key Laboratory of Catalysis in Dalian Institute of Chemical Physics, were named as Catal-A,[12] Catal-B, and Catal-C, respectively. Catal-A with transition metal nanoparticles Ru deposited on the outside wall of carbon nantubes was prereduced in a flow of H_2 at 450 °C for 12 h. After being packed into the microreactor, it was further online activated in H_2 flow with 50 mL min^{-1} from 30 to 200 °C for 60 min, from 200 to 300 °C at 5 °C min^{-1}, and finally at 300 °C for 60 min. Catal-B and Catal-C were prepared with same transition metal precursor and carbon nanotubes in two different methods, yielding two different types of structures.[43,44] Before the microcatalytic reaction, Catal-B and Catal-C were both online reduced by H_2 from room temperature to 550 °C with a heating rate of 4 °C min^{-1} and then held at 550 °C for 2 h.

RESULTS AND DISCUSSION

Ionization of NH_3 in SPI and CTI Modes. As NH_3 (IE = 10.07 eV) can be ionized both in SPI and CTI modes, 25 ppmv NH_3 in N_2/H_2 1:3 (vol) was tested, and the mass spectra are

dx.doi.org/10.1021/ac501576f | Anal. Chem. 2014, 86, 7681−7687

illustrated in Figure 2a and b, respectively. In SPI mode, the peak intensity of the NH_3^+ ions was only 713 counts when V_{SE1} was 30 V; however, in CTI mode, the peak intensity of the NH_3^+ ions dramatically increased to 74169 counts when V_{SE1} was 180 V, and the sensitivity is improved by about 100-fold. Therefore, CTI mode was employed in the next experiments for better sensitivity. On the basis of eq 7, sensitivity can be improved by increasing the number density of the O_2^+ ions in CTI mode.

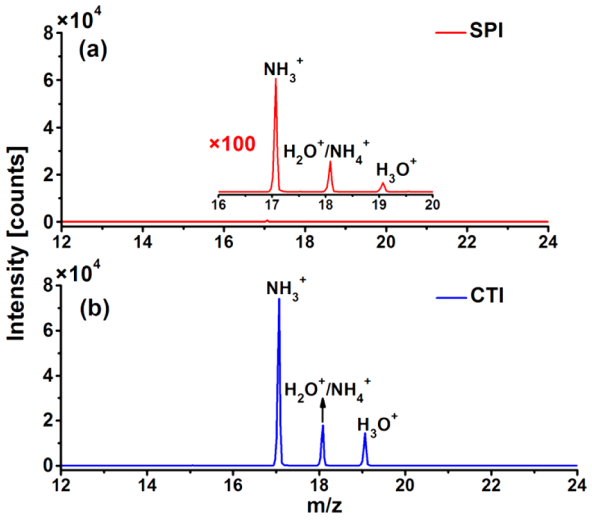

Figure 2. (a) Mass spectrum of 25 ppmv NH_3 in N_2/H_2 1:3 (vol) in SPI mode when V_{SE1} was set at 30 V. (b) Mass spectrum of 25 ppmv NH_3 in N_2/H_2 1:3 (vol) in CTI mode when V_{SE1} was set at 180 V.

Algorithm to Stabilize the Intensity of O_2^+ Reagent Ions. According to eq 7, the number density of the NH_3^+ ions exiting from the ion source, $[NH_3^+]_{t_r}$, is influenced by the number density of the O_2^+ ions exiting from the ion source $[O_2^+]_{t_r}$. Figure 3a shows the intensity variations of the O_2^+ ions and NH_3^+ ions when V_{SE1} is fixed at 70 V. The relative standard deviations (RSDs) of the O_2^+ and NH_3^+ intensities were 3.34% and 8.44%, respectively. Therefore, it is necessary to stabilize $[O_2^+]_{t_r}$ for accurate measurement of NH_3 at a certain concentration. In our CTI-MS, $[O_2^+]_{t_r}$ is affected by the number density of the O_2 reagent molecules, the VUV photon flux, the photoelectron emission efficiency of the electrode and the number density of the NH_3 molecules. The number density of the O_2 reagent molecules is always constant in our experiment. The VUV photon flux and the photoelectron emission efficiency of the electrode may decrease due to contamination of the VUV lamp and oxidation of the electrode during long-term measurement. For a high concentration of the NH_3 molecules up to thousands of ppmv, $[O_2^+]_{t_r}$ may decrease so significantly that accurate quantification of NH_3 fails to obtain.

Figure 3b displays the correlation between the peak intensity of the O_2^+ ions and the value of V_{SE1}. The peak intensity of the O_2^+ ions increased from 10 886 counts to 738 157 counts with an enhancement of more than 60-fold when V_{SE1} was changed from 40 to 200 V. Obviously, it is an effective solution to compensate the decay of the peak intensity of the O_2^+ ions by elevating the value of V_{SE1}. Therefore, we designed an algorithm

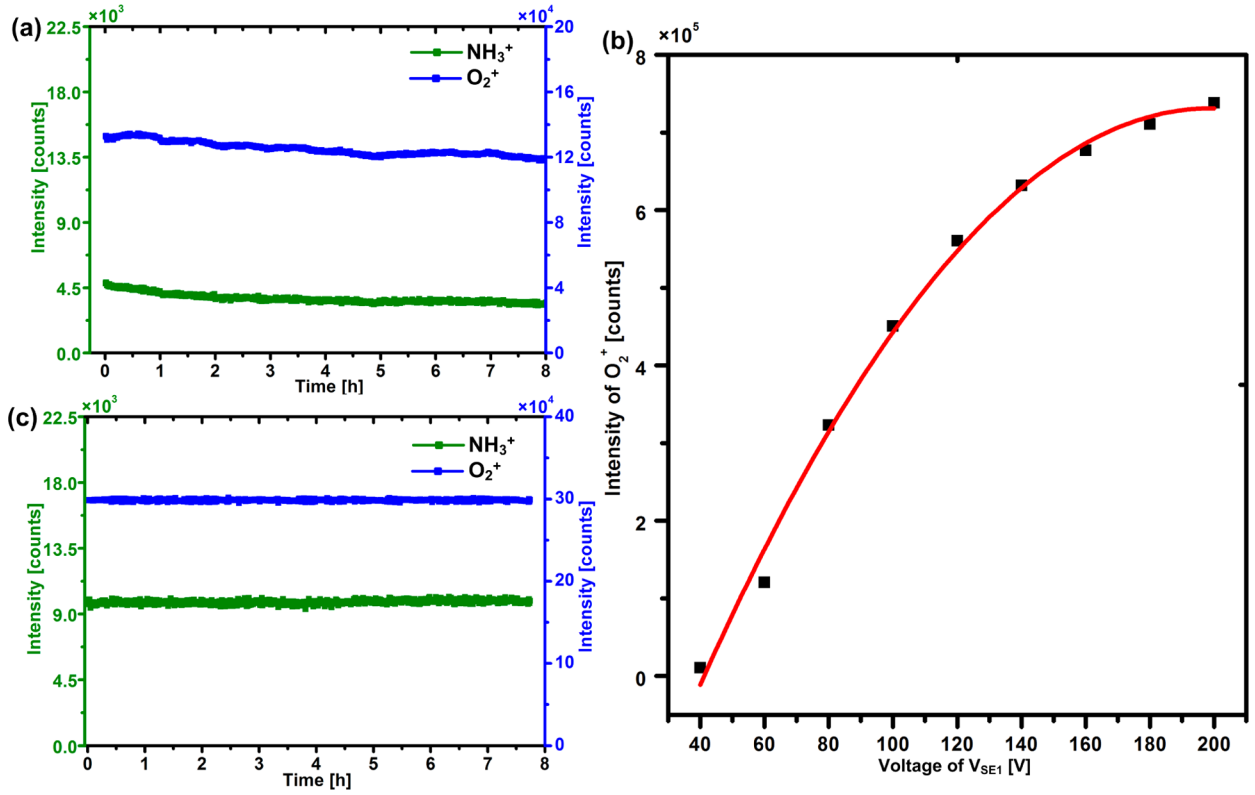

Figure 3. (a) Peak intensity profiles of the O_2^+ and NH_3^+ ions of 25 ppmv NH_3 in CTI mode without the algorithm. (b) Peak intensity of the O_2^+ reagent ions at different values of V_{SE1} in CTI mode. (c) Peak intensity profiles of the O_2^+ and NH_3^+ ions of 25 ppmv NH_3 in CTI mode after presetting O_2^+ intensity at 300 000 counts by the algorithm.

dx.doi.org/10.1021/ac501576f | Anal. Chem. 2014, 86, 7681−7687

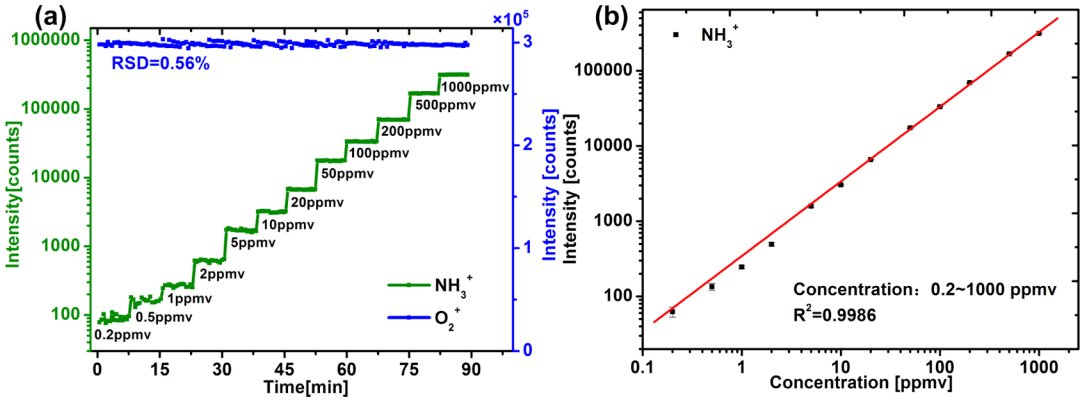

Figure 4. (a) Peak intensities of the NH_3^+ ions in N_2/H_2 1:3 (vol) at different concentrations in CTI mode. (b) Linear calibration curve for NH_3 in the concentration range from 0.2 ppmv to 1000 ppmv.

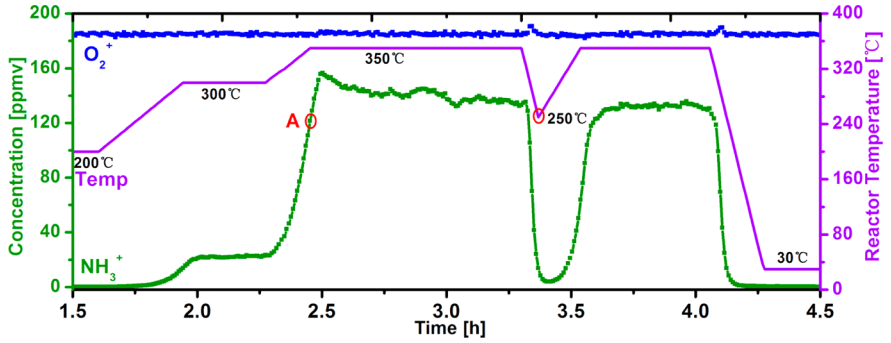

Figure 5. Time course of concentration of NH_3 in the outflow gas with Catal-A. Reaction conditions: catalyst, 100 mg; feed gas, N_2/H_2 1:3 (vol) with a flow rate of 20 mL min^{-1}; pressure, 0.1 MPa.

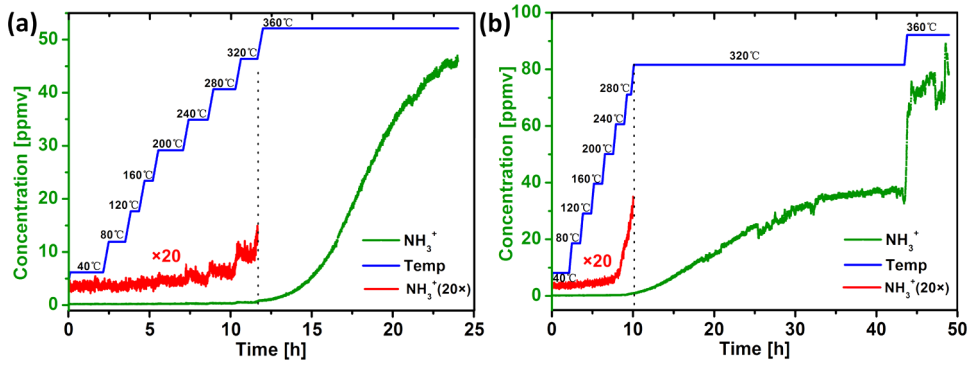

Figure 6. Time courses of concentration of NH_3 in the outflow gas with (a) Catal-B and (b) Catal-C. Reaction conditions: catalyst, 100 mg; feed gas, N_2/H_2 1:3 (vol) with a flow rate of 20 mL min^{-1}; pressure, 0.1 MPa.

to stabilize the intensity of the O_2^+ ions by automatically adjusting the value of V_{SE1}. With the algorithm, the present value of V_{SE1} is adjusted by comparing the O_2^+ intensity of the previous measurement cycle (30 s) with the preset O_2^+ intensity, the simplified principle is expressed as follows:

$$V_{n+1} = V_n + \eta\left(1 - \frac{I_n}{I_0}\right)V_n \ (n = 1, 2, 3...) \tag{9}$$

where n is the number of the measurement cycle, V_{n+1} is defined as the present value of V_{SE1} required, V_n is equivalent to the previous value of V_{SE1}, I_0 (counts) is the preset intensity of the O_2^+ ions, I_n (counts) represents the O_2^+ ion intensity of the previous measurement cycle, and η is the calibration coefficient.

Figure 3c depicts the intensity variation of 25 ppmv NH_3 during 8 h of continuous measurement stabilizing the O_2^+ reagent ions at 300 000 counts with the algorithm. The greatest variation between the measured and the preset O_2^+ intensity was 1.65%. The RSDs of the O_2^+ and NH_3^+ intensities were 0.38% and 1.3%, respectively. So, the following measurements were all performed with the above algorithm, and the O_2^+ ion intensity was fixed at 300 000 counts to facilitate long-term accurate quantitative measurement of ammonia.

Limit of Quantification (LOQ) and Linear Dynamic Range. Figure 4a displays continuous monitoring of NH_3^+ ion intensity at different concentrations of NH_3. The weak background signal at m/z = 17 was 30 counts accumulated in 30 s, which may result from the ionization of feed gas N_2/H_2 1:3 (vol) or permeation of atmospheric ammonia (~100 ppbv)

dx.doi.org/10.1021/ac501576f | Anal. Chem. 2014, 86, 7681−7687

into the instrument through polytetrafluoroethylene (PTFE) tubes.[21] The step-by-step intensity response of NH_3^+ with the increased NH_3 concentration reflected that the dead time and memory effect were small and negligible. The RSDs at different concentrations ranged from 0.5% (1000 ppmv) to 11% (0.2 ppmv), which revealed good precision. Figure 4b represents the calibration curve of the NH_3^+ ions, and almost 4 orders of magnitude dynamic range was obtained from 0.2 ppmv to 1000 ppmv with a good linear correlation coefficient (R^2 = 0.9986). Based on the S/N = 10 criteria, the LOQ for NH_3 is calculated to be 76 ppbv, which is adequate for online analysis of NH_3 in microcatalytic reactions. On the basis of eq 7, the stable quantitative performance and wide linear dynamic range of the current method were attributed to the stabilization of O_2^+ ion intensity and small variation of D_e with the upward concentration of NH_3 molecules.

Applications in Monitoring of Three Microcatalytic Synthesis Reactions. Figure 5 and Figure 6 depict the profiles of NH_3 concentration (in ppmv) in the effluent from the microreactor with three different catalysts.

In Figure 5, the Catal-A was first used to evaluate the quantitative performance of the CTI-TOFMS method on monitoring the concentration of NH_3 in the microcatalytic synthesis. The concentration of NH_3 started to increase rapidly around 255 °C, and an equilibrium concentration of 22 ppmv was achieved after the temperature was kept at 300 °C for 5 min. Then, the concentration of NH_3 reached a peak value of 155.7 ppmv shortly after the microreactor was heated to 350 °C (at point A) and decreased slowly to an equilibrium concentration of 134 ppmv. Part of NH_3 at the peak concentration was presumed to come from desorption of NH_3 previously formed at lower temperatures. The microreactor was cooled down to 250 °C with a rate of 25 °C min^{-1} after being kept for 51 min at 350 °C, and the microreactor was then immediately heated back to 350 °C with a rate of 10 °C min^{-1}. The rapid changes of NH_3 concentration according to temperature variations were clearly recorded. For example, the concentration of ammonia reached the same equilibrium value of 134 ppmv in 10 min after the temperature of the microreactor reached 350 °C again, and then the concentration of ammonia decreased to the baseline in 13 min after the reactor was cooled to ambient temperature. Catal-A exhibited stable catalytic activity, as there was no equilibrium concentration difference between the first temperature condition of 350 °C and the second one. The above results indicate good repeatability and reliability of the current CTI-TOFMS method.

Figure 6a,b show the concentration variation of NH_3 in the effluent gas with time at different temperatures using two catalysts (a) Catal-B and (b) Catal-C. As shown in Figure 6a, relative low equilibrium concentrations of NH_3 for Catal-B were achieved quickly between 40 and 320 °C, whereas it took about 12.3 h to reach the equilibrium concentration of 46 ppmv at 360 °C. From Figure 6b, we can see that there was no NH_3 observed below 240 °C, the concentration of NH_3 started to increase from 240 °C, and an equilibrium concentration of 37 ppmv at 320 °C was achieved more than 33 h later. However, the concentration of NH_3 reached its equilibrium value of 75 ppmv at 360 °C in only less than 32 min. Besides, there were obvious variations of conversion rate of NH_3 observed especially between the 25th hour and the 35th hour at 320 °C, and the variations became significant at 360 °C, which suggest the activity variations of Catal-C at corresponding temperatures.

The equilibrium conversion rates of NH_3, which is used to evaluate the catalytic activity of the investigated catalysts, can be calculated directly from the amount of catalyst, the flow rate, and the measured equilibrium concentration of NH_3 in the effluent gas. The conversion rates of NH_3 for Catal-B were 3.67 × 10^{-4} mol g^{-1} h^{-1} at 320 °C and 3.30 × 10^{-2} mol g^{-1} h^{-1} at 360 °C; however, those for Catal-C were 2.69 × 10^{-2} mol g^{-1} h^{-1} at 320 °C and 5.50 × 10^{-2} mol g^{-1} h^{-1} at 360 °C, respectively.

In summary, the concentration of synthesized NH_3 with low conversion rates under moderate conditions can be obtained in real-time with the highly sensitive CTI-TOFMS. The high-time-resolution continuous monitoring of the microreactions could acquire the activity changes of the studied catalysts in catalysis process. It should be noticed that the RSDs of the O_2^+ ion intensity were all smaller than 0.5% during the microcatalytic reactions, which implies excellent stability of the CTI-TOFMS method with the self-adjustment algorithm.

CONCLUSION

In this study, a high-sensitivity and high-time-resolution CTI-TOFMS method was presented for long-term real-time monitoring of ammonia during microcatalytic synthesis reaction with a time resolution of 30 s. A self-adjustment algorithm was used to stabilize the peak intensity of O_2^+ ions in the VUV-lamp-based CTI ion source for accurate quantification and wide linear dynamic range (0.2−1000 ppmv) during long-term monitoring. The microcatalytic reaction of feed gas N_2/H_2 1:3 (vol) with three different catalysts prepared by transition-metal/carbon nanotubes were tested, and the rapid changes of NH_3 conversion rates with the reaction temperatures were monitored with a time resolution of 30 s. The high-time-resolution monitoring data indicates that CTI-TOFMS can obtain the equilibrium conversion rates of NH_3 rapidly and provide information about the activity of investigated catalysts during catalytic reaction process.

Combined with intelligent self-adjustment and proper preset intensity of the reagent ions, the high time resolution of CTI-TOFMS provides a promising tool for long-term monitoring of various reaction processes besides ammonia microcatalytic synthesis reaction. With the technique, not only the conversion rates of the products but also the information on product distribution at different reaction stages can be acquired to evaluate the activities of the studied catalysts and to explore the reaction mechanism and pathways.

ASSOCIATED CONTENT

Supporting Information

Additional information as noted in the text. This material is available free of charge via the Internet at http://pubs.acs.org/.

AUTHOR INFORMATION

Corresponding Author

*E-mail: hli@dicp.ac.cn. Fax: +86-411-84379517.

Notes

The authors declare no competing financial interest.

ACKNOWLEDGMENTS

This work is partially supported by the National Special Fund for the Development of Major Research Equipment and

Instrument (grant no. 2013YQ09070302) and NSF of China (grant nos. 21375129, 21207129).

REFERENCES

(1) Ken-ichi, A.; Humio, H.; Ozaki, A. *J. Catal.* **1972**, *27*, 424.
(2) Ertl, G. *Angew. Chem., Int. Ed.* **2008**, *47*, 3524.
(3) Gruber, N.; Galloway, J. N. *Nature* **2008**, *451*, 293.
(4) Rafiqul, I.; Weber, C.; Lehmann, B.; Voss, A. *Energy* **2005**, *30*, 2487.
(5) Yandulov, D. V.; Schrock, R. R. *Science* **2003**, *301*, 76.
(6) Arashiba, K.; Miyake, Y.; Nishibayashi, Y. *Nat. Chem.* **2011**, *3*, 120.
(7) Lancaster, K. M.; Roemelt, M.; Ettenhuber, P.; Hu, Y.; Ribbe, M. W.; Neese, F.; Bergmann, U.; DeBeer, S. *Science* **2011**, *334*, 974.
(8) Lukoyanov, D.; Dikanov, S. A.; Yang, Z. Y.; Barney, B. M.; Samoilova, R. I.; Narasimhulu, K. V.; Dean, D. R.; Seefeldt, L. C.; Hoffman, B. M. *J. Am. Chem. Soc.* **2011**, *133*, 11655.
(9) Spatzal, T.; Aksoyoglu, M.; Zhang, L.; Andrade, S.; Schleicher, E.; Weber, S.; Rees, D.; Einsle, O. *Science* **2011**, *334*, 940.
(10) Kitano, M.; Inoue, Y.; Yamazaki, Y.; Hayashi, F.; Kanbara, S.; Matsuishi, S.; Yokoyama, T.; Kim, S.-W.; Hara, M.; Hosono, H. *Nat. Chem.* **2012**, *11*, 934.
(11) Tanabe, Y.; Nishibayashi, Y. *Coord. Chem. Rev.* **2013**, *257*, 2551.
(12) Guo, S.; Pan, X.; Gao, H.; Yang, Z.; Zhao, J.; Bao, X. *Chem.—Eur. J.* **2010**, *16*, 5379.
(13) Lin, B.; Wei, K.; Ni, J.; Lin, J. *ChemCatChem* **2013**, *5*, 1941.
(14) Fabris, D. *Mass Spectrom. Rev.* **2005**, *24*, 30.
(15) Jin, W.; Zhang, C.; Chang, X.; Fan, Y.; Xing, W.; Xu, N. *Environ. Sci. Technol.* **2008**, *42*, 3064.
(16) Martha, C. T.; Elders, N.; Krabbe, J. G.; Kool, J.; Niessen, W. M. A.; Orru, R. V. A.; Irth, H. *Anal. Chem.* **2008**, *80*, 7121.
(17) Paz-Schmidt, R. A.; Bonrath, W.; Plattner, D. A. *Anal. Chem.* **2009**, *81*, 3665.
(18) Melligan, F.; Hayes, M. H. B.; Kwapinski, W.; Leahy, J. J. *Energy Fuels* **2012**, *26*, 6080.
(19) NIST National Institute of Standards and Technology (NIST). http://webbook.nist.gov/chemistry/ (accessed April 10, 2014).
(20) Hanson, D. R.; McMurry, P. H.; Jiang, J.; Tanner, D.; Huey, L. G. *Environ. Sci. Technol.* **2011**, *45*, 8881.
(21) Norman, M.; Hansel, A.; Wisthaler, A. *Int. J. Mass Spectrom.* **2007**, *265*, 382.
(22) Trefz, P.; Schmidt, M.; Oertel, P.; Obermeier, J.; Brock, B.; Kamysek, S.; Dunkl, J.; Zimmermann, R.; Schubert, J. K.; Miekisch, W. *Anal. Chem.* **2013**, *85*, 10321.
(23) Eschner, M. S.; Groger, T. M.; Horvath, T.; Gonin, M.; Zimmermann, R. *Anal. Chem.* **2011**, *83*, 3865.
(24) Geissler, R.; Saraji-Bozorgzad, M. R.; ger, T. G.; Fendt, A.; Streibel, T.; Sklorz, M.; Krooss, B. M.; Fuhrer, K.; Gonin, M.; Kaisersberger, E.; Denner, T.; Zimmermann, R. *Anal. Chem.* **2009**, *81*, 6038.
(25) Eschner, M. S.; Selmani, I.; Groger, T. M.; Zimmermann, R. *Anal. Chem.* **2011**, *83*, 6619.
(26) Streibel, T.; Mitschke, S.; Adam, T.; Zimmermann, R. *Anal. Bioanal. Chem.* **2013**, *405*, 7071.
(27) Hua, L.; Wu, Q.; Hou, K.; Cui, H.; Chen, P.; Wang, W.; Li, J.; Li, H. *Anal. Chem.* **2011**, *83*, 5309.
(28) Wu, Q.; Hua, L.; Hou, K.; Cui, H.; Chen, W.; Chen, P.; Wang, W.; Li, J.; Li, H. *Anal. Chem.* **2011**, *83*, 8992.
(29) Hou, K.; Li, F.; Chen, W.; Chen, P.; Xie, Y.; Zhao, W.; Hua, L.; Pei, K.; Li, H. *Analyst* **2013**, *138*, 5826.
(30) Watanabe, K. *J. Chem. Phys.* **1954**, *22*, 1564.
(31) Kuribayashi, S.; Yamakoshi, H.; Danno, M.; Sakai, S.; Tsuruga, S.; Futami, H.; Morii, S. *Anal. Chem.* **2005**, *77*, 1007.
(32) Chen, P.; Hou, K.; Hua, L.; Xie, Y.; Zhao, W.; Chen, W.; Chen, C.; Li, H. *Anal. Chem.* **2014**, *86*, 1332.
(33) Sintermann, J.; Ammann, C.; Kuhn, U.; Spirig, C.; Hirschberger, R.; Gärtner, A.; Neftel, A. *Atmos. Meas. Tech.* **2011**, *4*, 1821.
(34) Sintermann, J.; Spirig, C.; Jordan, A.; Kuhn, U.; Ammann, C.; Neftel, A. *Atmos. Meas. Tech.* **2011**, *4*, 599.
(35) Schmitz, T. A.; Gamez, G.; Setz, P. D.; Zhu, L.; Zenobi, R. *Anal. Chem.* **2008**, *80*, 6537.
(36) Wu, Q.; Hua, L.; Hou, K.; Cui, H.; Chen, P.; Wang, W.; Li, J.; Li, H. *Int. J. Mass Spectrom.* **2010**, *295*, 60.
(37) Španěl, P.; Smith, D. *Med. Biol. Eng. Comput.* **1996**, *34*, 409.
(38) RAKSIT, A. B. *Int. J. Mass Spectrom. Ion Processes* **1986**, *69*, 45.
(39) Dryahina, K.; Španěl, P. *Int. J. Mass Spectrom.* **2005**, *244*, 148.
(40) Španěl, P.; Dryahina, K.; Smith, D. *Int. J. Mass Spectrom.* **2006**, *249*, 230.
(41) Smith, D.; Spanel, P. *Mass Spectrom Rev.* **2005**, *24*, 661.
(42) Baumbach, J. I. E.; Gary, A. *Appl. Spectrosc.* **1999**, *53*, 338A.
(43) Hayashi, F.; Iwamoto, M. *Microporous Mesoporous Mater.* **2011**, *146*, 184.
(44) Seipenbusch, M.; Binder, A. *J. Phys. Chem. C* **2009**, *113*, 20606.